Analyst

PAPER

Cite this: *Analyst*, 2016, **141**, 4438

# Ion mobility spectrometry nuisance alarm threshold analysis for illicit narcotics based on environmental background and a ROC-curve approach†‡

Thomas P. Forbes* and Marcela Najarro

The discriminative potential of an ion mobility spectrometer (IMS) for trace detection of illicit narcotics relative to environmental background was investigated with a receiver operating characteristic (ROC) curve framework. The IMS response of cocaine, heroin, methamphetamine, 3,4-methylenedioxymethamphetamine (MDMA), and $\Delta^9$-tetrahydro-cannabinol (THC) was evaluated against environmental background levels derived from the screening of incoming delivery vehicles at a federal facility. Over 20 000 samples were collected over a multiyear period under two distinct sets of instrument operating conditions, a baseline mode and an increased desorption/drift tube temperature and sampling time mode. ROC curves provided a quantifiable representation of the interplay between sensitivity (true positive rate, TPR) and specificity (1 – false positive rate, FPR). A TPR of 90% and minimized FPR were targeted as the detection limits of IMS for the selected narcotics. MDMA, THC, and cocaine demonstrated single nanogram sensitivity at 90% TPR and <10% FPR, with improvements to both MDMA and cocaine in the elevated temperature/increased sampling mode. Detection limits in the tens of nanograms with poor specificity (FPR ≈ 20%) were observed for methamphetamine and heroin under baseline conditions. However, elevating the temperature reduced the background in the methamphetamine window, drastically improving its response (90% TPR and 3.8% FPR at 1 ng). On the contrary, the altered mode conditions increased the level of background for THC and heroin, partially offsetting observed enhancements to desorption. The presented framework demonstrated the significant effect environmental background distributions have on sensitivity and specificity.

Received 11th April 2016,
Accepted 18th May 2016

DOI: 10.1039/c6an00844e

www.rsc.org/analyst

## Introduction

The rapid and sensitive detection of illicit narcotics remains vital to a multitude of law enforcement, corrections/prisons, customs and border protection, and transportation agencies. Laboratory-based analytical techniques including thin-layer chromatography (TLC),[1,2] gas and liquid chromatography (GC, LC),[3–7] capillary electrophoresis (CE),[8,9] and mass spectrometry (MS)[10–14] have been developed and utilized for the detection of a wide range of narcotic compounds. However, many of these techniques require additional laboratory infrastructure and are not conducive to field deployment or point-of-measurement screening. Colorimetric methods for the detection of narcotics have been developed and provide rapid detection in the field.[15,16] However, these presumptive tests are subject to screener interpretation of the resulting color(s) and require on-site reagent mixing.

In recent years, ion mobility spectrometry (IMS) has surged forward as a robust field-deployable analytical technique for the trace detection of a wide range of compounds, most notably explosives,[17–21] chemical warfare agents (CWAs),[22–24] and illicit narcotics.[25–28] Typically, IMS utilizes thermal desorption for the volatilization of collected analyte; followed by gas-phase ionization through reactions with a $^{63}$Nickel radiation source ($^{63}$Ni), photoionization, or corona discharge chemical ionization; and finally separation based on electric mobility through a drift cell. These instruments have been developed for easy operation by non-technical personnel, with tens of thousands (and continually increasing) units deployed worldwide to combat movement of contraband materials and mitigate threats.[29,30]

*National Institute of Standards and Technology, Materials Measurement Science Division, Gaithersburg, MD, USA. E-mail: thomas.forbes@nist.gov*



‡Electronic supplementary information (ESI) available: Additional experimental details, raw data, IMS spectra, and figures as noted in the text. See DOI: 10.1039/c6an00844e

Ion mobility spectrometry has demonstrated sensitive detection (limits of detection on the order of picograms to nanograms),[31] however, it suffers from limitations in selectivity and peak resolution,[32] as well as signal saturation.[26] Most commercial instruments are equipped with a library of known target analytes and specified alarm threshold intensity levels. Environmental background and contaminants can result in ions with similar drift times to target analytes. Limitations in peak differentiation can lead to reduced specificity and an increase in the rate of false positive alarms. These threshold levels are very much analyte and application specific, and a function of the relative true positive and false positive alarm rates required. Receiver operating characteristic (ROC) curves, introduced during World War II, can be used to graphically represent the relative sensitivity and specificity of a sensor/instrument as a function of specific parameters.[33–36] ROC curves were originally developed to evaluate radar signals; however, they have been utilized in a wide range of fields, with their most notable popularity in clinical diagnostics.[37–43] The classical ROC curve plots the true positive rate (TPR: sensitivity) against the false positive rate (FPR: 1 – specificity) for a dichotomous system. In the case of a chemical sensor, *i.e.*, IMS, this manifests as either an alarm signifying the presence of a target (positive) or the lack thereof signifying the absence of the target (negative). The curve is generated by varying the specified threshold intensity for an alarm, enabling the appropriate threshold to be chosen based on the resulting sensitivity/specificity tradeoff. Recently, the Defense Advanced Research Projects Agency (DARPA) of the U.S. Department of Defense also proposed the use of ROC curves to investigate chemical and biological sensors.[44] These recommendations have been utilized directly to evaluate CWA detection by atmospheric pressure ionization mass spectrometry[33] and in the development of a portable mass spectrometer.[35]

In the present investigation, we incorporate ROC curves for the evaluation of nuisance alarm thresholds of illicit narcotics using ion mobility spectrometry. The detection of five illicit narcotics (cocaine, heroin, methamphetamine (METH), 3,4-methylenedioxymethamphetamine (MDMA), and $\Delta^9$-tetrahydrocannabinol (THC)) was investigated using two commercial ion mobility spectrometers (IMS). The response (*i.e.*, signal intensity, alarm threshold, TPR, and FPR) of each narcotic was evaluated against environmental background levels derived from over 20 000 samples collected over a multiyear period from an instrument deployed at a federal facility for the screening of incoming delivery vehicles. The environmental background samples were used to measure the baseline level of background at each target analyte's drift time, including noise, environmental contaminants (other compounds with the same/similar drift time), and background levels of the target narcotic. This accounted for instances similar to the background levels of cocaine on U.S paper currency[45] or drugs of abuse in airborne particles.[46–48] The detection response for each narcotic was characterized using a ROC curve analysis, varying a number of IMS-system (desorber/drift tube temperatures and sampling time) and analysis (alarm threshold, target drift time window, analyte mass) parameters. The overall detection of the illicit narcotics was a strong function of the analyte and its vapor pressure/potential for thermal desorption. However, the frequency and intensity of the environmental background played a more significant role in discrimination potential of IMS between target narcotic and background.

## Experimental methods/materials and methods

### Ion mobility spectrometer(s)

The experiments reported here were conducted on two ion mobility spectrometers (IMS) manufactured by Morpho Detection, LLC (Safran Group). These instruments utilized an ion trap mode of operation, in which ions are allowed to accumulate in the reaction region before being pulsed into the drift region.[18,49–51] This configuration eliminates the losses due to cycling of the gating grid electrode in classical IMS. Here, an IMS instrument deployed for the field screening of incoming delivery trucks at a federal facility was positioned at a loading dock with no specific control over environmental conditions. A second laboratory-based instrument was housed within the Advanced Measurement Laboratory at NIST. The IMS instruments contained a thermal desorber for gas phase introduction of analyte(s) directly from swab/swipe substrates, a $^{63}$Ni radiation source for analyte ionization, and a faraday plate for ion detection. Ionization was achieved in conjunction with a doped reactant, ammonia or dichloromethane, and the respective positive and negative mode product ions. The IMS hardware configuration enabled simultaneous analysis of positive and negative modes by sequentially cycling between positive and negative polarity during the sampling period. The instruments were operated under two sets of conditions based on manufacturer recommended parameters, a base case mode (Mode 1) and an elevated desorption/drift tube temperature and increased sampling time mode (Mode 2), listed in Table 1, for the presented experiments.

Certain commercial products are identified in order to adequately specify the procedure; this does not imply endorsement or recommendation by NIST, nor does it imply that such products are necessarily the best available for the purpose.

### Materials and sample preparation/collection

Narcotic standards, including cocaine (CAS number 50-36-2), heroin (CAS no. 561-27-3), methamphetamine (METH, CAS no.

Table 1 Parameters for the IMS instrument modes of operation

| IMS parameter | Mode 1 | Mode 2 |
|---|---|---|
| Desorber temperature (°C) | 220 | 235 |
| Detection/tube temperature (°C) | 163 | 202 |
| Drift flow ($cm^3$ $min^{-1}$) | 100 | 100 |
| Sample flow ($cm^3$ $min^{-1}$) | 50 | 50 |
| Sampling time (s) | 8 | 13 |

7632-10-2), 3,4-methylenedioxymethamphetamine (MDMA, CAS no. 42542-10-9), and $\Delta^9$-tetrahydrocannabinol (THC, CAS no. 1972-08-3), were purchased from Cerilliant (Round Rock, TX, USA) in base form at 1 mg $mL^{-1}$ in methanol or acetonitrile and further diluted as required in liquid chromatography-mass spectrometry (LC-MS) Chromasolv grade acetonitrile (Sigma-Aldrich, St. Louis, MO, USA). For verification measurements on the deployed and laboratory experiments, samples of 200 pg to 200 ng were solution deposited onto polytetrafluoroethylene (PTFE)-coated fiberglass swabs (Sample Traps-ST1318, DSA Detection, LLC, Boston, MA, USA) and the solvent was allowed to evaporate before introduction into the IMS desorber. Field sample collection/screening was primarily conducted by swiping with a sampling wand (Morpho Detection, LLC, Newark, CA, USA); however, under high vehicular traffic volume conditions, a second screener used manual hand sampling in parallel. Sample collection from delivery vehicles comprised of common target areas, including, but not limited to, steering wheels, inside door latches, and gear shifters. All screening samples interrogated by the IMS instrument were archived at the time of collection and later retrieved for this study. A total of 18 504 samples were collected with the deployed instrument from December 2012 through September 2014 in the base case Mode 1 and 3293 samples from April 2015 through July 2015 in Mode 2.

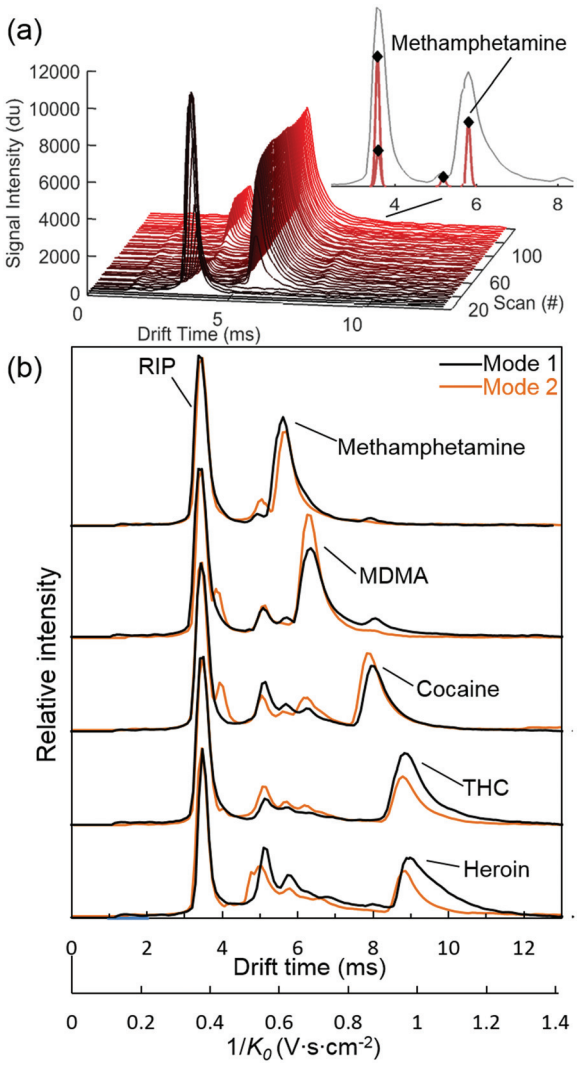


**Fig. 1** (a) IMS spectra across 120 scans for 10 ng methamphetamine in Mode 1. Inset represents the maximum adjusted amplitude across scans and the firmware identified peaks. (b) Representative raw IMS spectra across corresponding sampling times for select illicit narcotics in (—) Mode 1 (methamphetamine: 10 ng, MDMA: 10 ng, cocaine: 10 ng, THC: 10 ng, heroin: 200 ng) and (—) Mode 2 (methamphetamine: 5 ng, MDMA: 15 ng, cocaine: 5 ng, THC: 5 ng, heroin: 25 ng). All spectra intensities were normalized relative to the RIP (reactant ion peak) intensity value (peak height) seen at ≈ 3.4 ms ($K_0 \approx 2.71$ $cm^2$ $V^{-1}$ $s^{-1}$).

### Data processing

The IMS firmware digitally processed the raw signals (Fig. 1) based on proprietary algorithms that included a baseline correction and amplitude adjustment, followed by peak identification based on adjusted amplitude at maximum slope (with respect to scan number – Fig. 1(a)). It is important to note that the raw signal processing of the IMS firmware was utilized here for peak identification (Fig. 1(a) and S-1‡), however, the detection/alarm algorithms (also proprietary) were not. In addition, drift time calibration was conducted through the system firmware using external calibrants. The archived data files for all samples, processed with the IMS peak identification firmware, were collated and batch post-processed using a custom MATLAB-based code (MATLAB R2015a, Mathworks, Inc., Natick, MA, USA). Additional details of the calibration, calibrants, and data processing can be found in the ESI.‡

## Results and discussion

### Reduced mobilities

The laboratory instrument was utilized to measure the IMS response for the five illicit narcotics, including calibration corrected drift time ($t_d$) and reduced mobility ($K_0$), in each mode of operation. The drift times are often normalized to system (drift tube length and electric field) and environmental parameters (pressure and temperature), resulting in reduced mobilities.[53,54] Fig. 1 demonstrates representative raw IMS spectra for each of the narcotics in both modes, across the sampling time, as a function of drift time and corresponding inverse reduced mobility. These spectra were processed by the commercial firmware for peak identification (Fig. S-1‡).

Experimentally, the reduced mobility was calculated from the calibration corrected drift time using, $K_0 = (K_0 t_d)_{cal}/t_d$, where the subscript "*cal*" signifies the reduced mobility and drift time of the calibrant (cocaine in positive mode).[53,54] This expedited approach has been used often for commercial instruments. Table 2 provides the average drift times and reduced mobilities for the illicit narcotics from nominally 90 samples (actual totals range from 88 to 98), comprised of 30 replicates at 3 mass loadings, taken across a three-week period. As seen in Fig. 1 and Table 2, there were slight vari-

Table 2 Analyte properties including vapor pressure (VP; at 25 °C), calibration corrected drift times, and reduced mobilities (measured & literature) for illicit narcotics in Modes 1 and 2. Values in parentheses represent the standard deviation from nominally $n$ = 90 samples (30 replicates at three mass loadings)

| Analyte | Molecular weight (g mol$^{-1}$) | VP[a 52] (kPa) | Sample masses investigated (ng) | | Calibration corrected drift time (ms) | | $K_0$ measured (cm$^2$ V$^{-1}$ s$^{-1}$) | | $K_0$ literature[26] (cm$^2$ V$^{-1}$ s$^{-1}$) |
|---|---|---|---|---|---|---|---|---|---|
| | | | Mode 1 | Mode 2 | Mode 1 | Mode 2 | Mode 1 | Mode 2 | |
| METH | 149.24 | $2.17 \times 10^{-2}$ | 1, 5, 10 | 0.2, 1, 5 | 5.759 (0.027) | 5.680 (0.025) | 1.598 (0.008) | 1.621 (0.007) | 1.643 |
| MDMA | 193.25 | $2.13 \times 10^{-4}$ | 2, 6, 10 | 1, 5, 15 | 6.367 (0.035) | 6.322 (0.013) | 1.446 (0.008) | 1.456 (0.003) | 1.472 |
| Cocaine | 303.35 | $2.55 \times 10^{-8}$ | 2, 3, 10 | 0.5, 1, 5 | 7.941 (0.034) | 7.924 (0.013) | 1.159 (0.005) | 1.162 (0.002) | 1.164 |
| THC | 314.47 | $6.17 \times 10^{-9}$ | 2, 5, 10 | 0.5, 2, 5 | 8.774 (0.023) | 8.775 (0.018) | 1.049 (0.003) | 1.049 (0.002) | 1.050 |
| Heroin | 369.41 | $1.01 \times 10^{-10}$ | 10, 50, 200 | 2.5, 10, 25 | 8.856 (0.024) | 8.807 (0.017) | 1.039 (0.003) | 1.045 (0.002) | 1.046 |

[a] Estimated using EPI Suite™ v4.11, US EPA, 2014.

ations in the drift times between modes. This was not unexpected as the drift tube temperature plays a direct role in the drift time. The derived reduced mobilities were found to be comparable to those in the literature, measured on a different IMS instrument.[26] These variations were expected as a result of differences in the instrument design/geometry and system parameters.

The environmental background from screening of incoming delivery trucks across a multiyear period was assessed at the measured drift times/reduced mobilities (Table 2) to evaluate the appropriate IMS nuisance alarm (false positive) thresholds of illicit narcotics. Two fundamental assumptions were implemented for the completion of this analysis. First, the samples collected from delivery vehicles and measured on the deployed instrument were presumed and categorized as true negatives. In the context of this study, a true negative represented the environmental background levels and not necessarily the complete absence of the target analyte. This reasoning was employed to differentiate between target and background levels of the illicit narcotics. For example, previous studies have demonstrated that approximately 92% of U.S. paper currency is contaminated with significant levels (tens of micrograms) of cocaine,[45] however, that does not necessarily indicate the deliberate or criminal presence of cocaine by the holder of that currency. Therefore, the possibility for the unintentional presence of trace levels of these narcotics from collected samples was categorized as environmental background. In the context of this work, nuisance alarm and false positive were used interchangeably and included both the absence of the target analyte as well as responses at or below background levels.

As introduced above, the testing methodology and ROC curve development was derived from the DARPA study, "Chemical and Biological Sensor Standards Study".[44] Given the inability to release or deposit chemicals into the environment of interest, *e.g.*, private vehicles, the DARPA study advocates acquiring the target response under laboratory settings and background samples from a different applicable environment, and then combining the response data.[34,44] This methodology has been demonstrated with chemical/biological sensors and in the literature.[33,35] Following this methodology, a second underlying assumption was incorporated, specifically that measurements taken on either the laboratory or deployed instrument were transferable, *i.e.*, drift time measurements and sensitivities on the laboratory instrument translated to data collected on the deployed instrument. Both instruments were routinely calibrated in the same manner with the same calibrants, appropriately adjusting drift times. A subset of experiments (five replicates for select narcotics) were conducted on the deployed instrument and demonstrated matching drift times in both modes to the laboratory values reported in Table 2. In addition, the laboratory instrument's amplitude adjusted response to the calibrant was measured 25% higher than the deployed instrument and ~18% RSD across both instruments (less than the >30% RSDs for explosives RDX and PETN previously measured across multiple (16) deployed instruments).[21] Though ambient/environmental conditions of the deployed instrument have the potential to introduce variability in the IMS response and even the calibrant response, the calibration correction (Fig. S-2‡) and intensity (Fig. S-3 and S-4‡) for the instrument was monitored and remained relatively stable across the multiyear period of sample collection, showing no systematic drift in response. In addition, previous work comparing the responses of multiple deployed commercial instruments found no correlation between response and environmental conditions (*e.g.*, temperature or humidity).[21] Finally, previous long-term studies of laboratory and deployed instruments found response variability (relative standard deviation) was derived from the technology limitations and instrument manufacture, as opposed to environmental contamination.[21]

### Environmental background – true negatives

The deployed instrument collected 18 504 samples under Mode 1 operating conditions across a multiyear period, followed by an additional 3293 samples under Mode 2 conditions (Table 1). Mode 2 operation consisted of increased desorption/drift tube temperatures and sampling time (Table 1). Fig. 2 displays frequency histograms for IMS peaks identified at the calibrated drift time of the five illicit narcotics from samples collected during each experimental period (signal intensity given in digital units (du)). The default drift time window for target identification was ±0.05 ms, centered on the values in

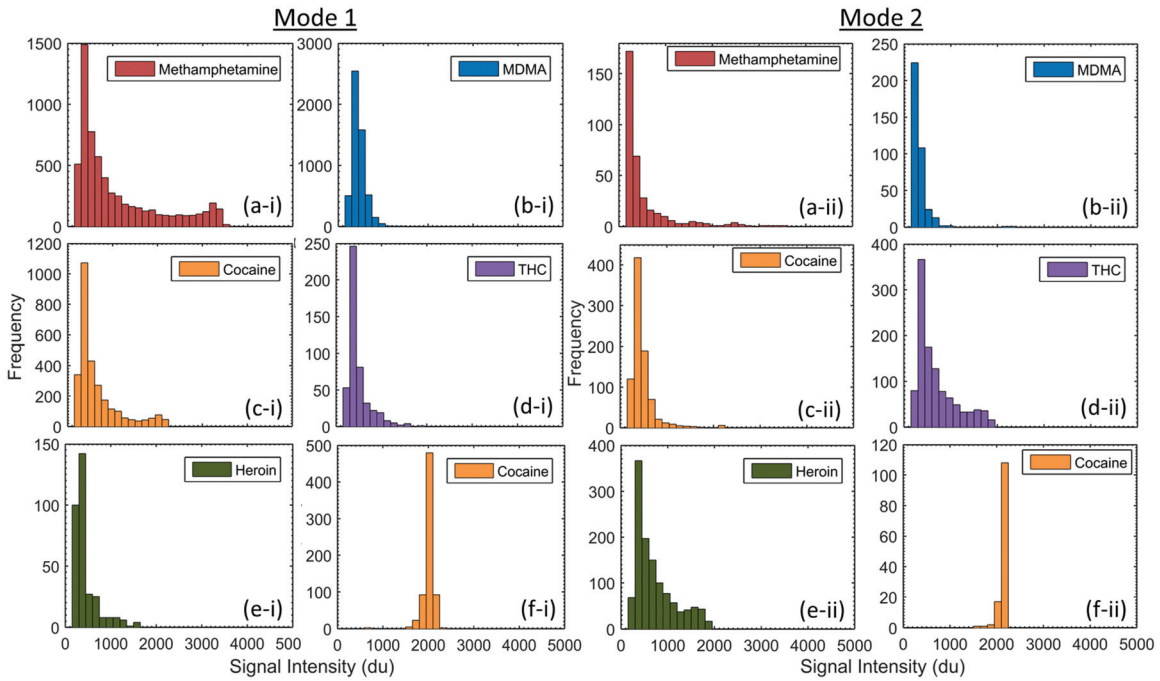


**Fig. 2** (a)–(e) Frequency histograms of background intensity data from the deployed IMS instrument in (i) Mode 1 for across a multiyear period (18 504 total files/samples) and (ii) Mode 2 for across a 3-month period (3293 total files/samples). Drift times measured on the laboratory instrument with a ±0.05 ms window were utilized here. (f) Frequency histograms for cocaine from the calibration files across each collection period (i – 739 calibrations, ii – 129 calibrations).

Table 2. The drift time window will be discussed further below. The results demonstrated variable distributions in terms of overall frequency and signal intensity for each of the narcotics, however, each narcotic exhibited similar distributions between Mode 1 and Mode 2 operation. There were relatively fewer peaks in the longer drift time range of THC and heroin as compared to the shorter drift time range of methamphetamine and MDMA in Mode 1. However, the increased desorption/drift tube temperatures and sampling time increased the relative number of background peaks in the longer drift time windows in Mode 2 (Fig. 2). This was most noticeable in the 1000 du to 2000 du range for THC and heroin (Fig. 2(d) and (e)). The general distributions were relatively consistent across both the multiyear period in Mode 1 (Fig. S-3‡) and multi-month period in Mode 2 (Fig. S-4‡), with neither demonstrating observable systematic drift. Fig. 2(f) displays the cocaine frequency histograms for calibration files across both periods, demonstrating a tight distribution around intensity of approximately 2000 du in Mode 1, and increase to 2200 du in Mode 2.

### Target response – true positives

Frequency histograms for the IMS response to the five illicit narcotics were measured under Mode 1 and Mode 2 operating conditions (Fig. S-5 and S-6‡). The response for each narcotic was measured at three mass loadings with nominally 30 replicates at each loading. Different loadings were investigated in each mode given the different system conditions (desorption/drift tube temperatures and sampling time) and corresponding different IMS response. As may be expected, the increased desorber temperature and sampling time improved the IMS response across the range of narcotics in Mode 2 (Fig. S-6‡). These data provided the corresponding drift time measurements in Table 2. The narcotics investigated here demonstrated variable IMS responses due to the physicochemical properties of each compound. As demonstrated (and most apparent at the high mass loading), the relative signal intensity decreased from methamphetamine down to heroin, corresponding to a decrease in compound vapor pressure/volatility (Fig. S-5 and S-6‡). Volatility was utilized here to provide a description of the material properties qualitatively encompassed in the desorption process including boiling points, sublimation rates, intermolecular forces, and surface adsorption.

As the narcotic molecules decreased in vapor pressure, and therefore volatility, the thermal desorption process was less effective/efficient at vaporizing the compound for ionization and analysis. The initiation of desorption and the duration of signal was a function of the volatility of each target. This was demonstrated comparing methamphetamine to cocaine, a six-order of magnitude difference in vapor pressure. For the desorber temperature (220 °C) in Mode 1 operation, the initial point of desorption for 10 ng of methamphetamine began approximately one second after sampling/thermal desorption was initiated and the signal persisted through the remainder of the 8 s sampling time (Fig. S-7‡). This rise in signal corres-

 

ponded directly with a consumption of the reactant ion and decrease in the RIP signal. However, cocaine desorption and corresponding signal was not observed until approximately 2.5 s after sampling was initiated and the cocaine signal only persisted for approximately 2.6 s (Fig. S-7‡). These trends were consistent across the range of compounds as a function of volatility and were also observed at the elevated desorber temperature (235 °C) in Mode 2 operation (Fig. S-8‡). Next, the IMS measurements of environmental background (Fig. 2) and target response (Fig. S-5 and S-6‡) were directly compared utilizing a ROC curve approach to evaluate the instrument's discriminative capabilities.

### ROC curves

The nuisance alarm thresholds were investigated using a ROC curve approach with environmental background levels measured across each operating mode period and the three (3) respective true positive target mass loadings. This method was utilized to demonstrate the operational trade-off between detection/sensitivity (TPR) and the instrument specificity (1-FPR). Here, we evaluated the alarm thresholds levels to appropriately differentiate between target and background levels of illicit narcotics. As introduced above, the data represented measurements across a range of environmental conditions, periods of time, and sample composition, providing a representative look at the IMS performance. For each ROC curve, the alarm threshold was varied from 0 du to 4000 du in 200 du increments, covering the complete demarcation of the environmental background displayed in Fig. 2. At each alarm threshold, specific TPR and FPR points were evaluated at each target mass loading and displayed as data points on the ROC curve. In these curves, the line from (0,0) to (1,1) represents the line of no discrimination, along which the IMS cannot discriminate between target and background.

The utility of ROC curves will be demonstrated for methamphetamine under Mode 1 conditions. The methamphetamine drift time exhibited significant background (Fig. 2(a–i)), resulting in limited discrimination (Fig. 3) in this mode. The IMS could not distinguish between the target and background above a threshold value ~1800 du for the lowest mass (1 ng) of methamphetamine (Fig. 3). In this range, the sensitivity (TPR) fell to 0%. This can also be visualized through the overlaid signal distributions (Fig. S-9(a)‡). However, as the alarm threshold was decreased (moving to the right on the ROC curve), the IMS under Mode 1 operating conditions discriminated between the target and background. For example, at a threshold of 1000 du, the IMS response resulted in ~0.9 TPR (90% TPR), however this corresponded to a ~0.36 FPR (36% FPR). Given the relatively strong background signal in the methamphetamine window, higher levels of false positives were observed. The discrimination between target and background improves as the ROC curves approaches the (0, 1) point. At the highest methamphetamine loading (10 ng) and a 2000 du threshold level, ~90% TPR and corresponding ~18% FPR was achieved (Fig. 3 and S-9(a)‡). The determination of the appropriate threshold with corresponding sensitivity and specificity is very much a function of the application, target, and user requirements.

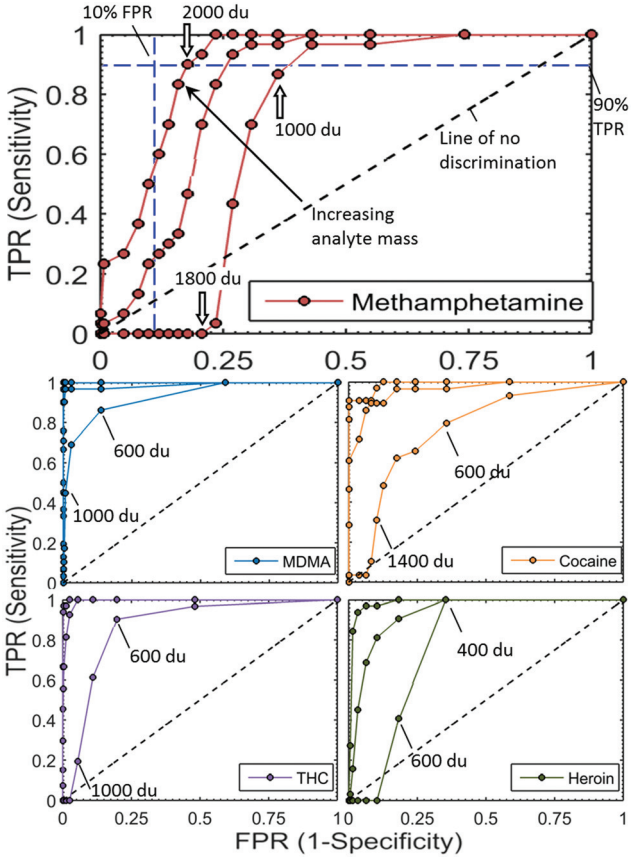


**Fig. 3** ROC curves for each target narcotic at three mass loading levels (methamphetamine: (1, 5, 10) ng, MDMA: (2, 6, 10) ng, cocaine: (2, 3, 10) ng, THC: (2, 5, 10) ng, and heroin: (10, 50, 200) ng) for IMS operating in Mode 1 with a ±0.05 ms drift time window. Nuisance/alarm thresholds were varied from 0 du to 4000 du in 200 du increments. The line from (0,0) to (1,1) represents the line of no discrimination. Lines of 90% TPR and 10% FPR are labeled on the methamphetamine ROC curves, as well as various thresholds on each narcotic ROC curves for reference.

Fig. 4 represents ROC curves under Mode 2 operating conditions. Differences in mass aside, the IMS performance (based on the ROC curves) differed significantly between Mode 1 and Mode 2 operation. For example, Under Mode 2 conditions, the environmental background in the methamphetamine window was skewed toward lower intensity and led to improved sensitivity and specificity as demonstrated in Fig. 5. While the increase in desorption temperature and sampling time improved the pure analyte response across the board (Fig. S-6‡), and significantly for the low volatility compounds, it also increased the level of environmental background peaks in the drift time windows of those compounds. The noticeable increase in the frequency and intensity of background peaks at the drift time window for THC corresponded to an increase in the FPR, pushing the ROC curves to the right, decreasing overall IMS discrimination capability between target and environmental background. This was clearly demonstrated by

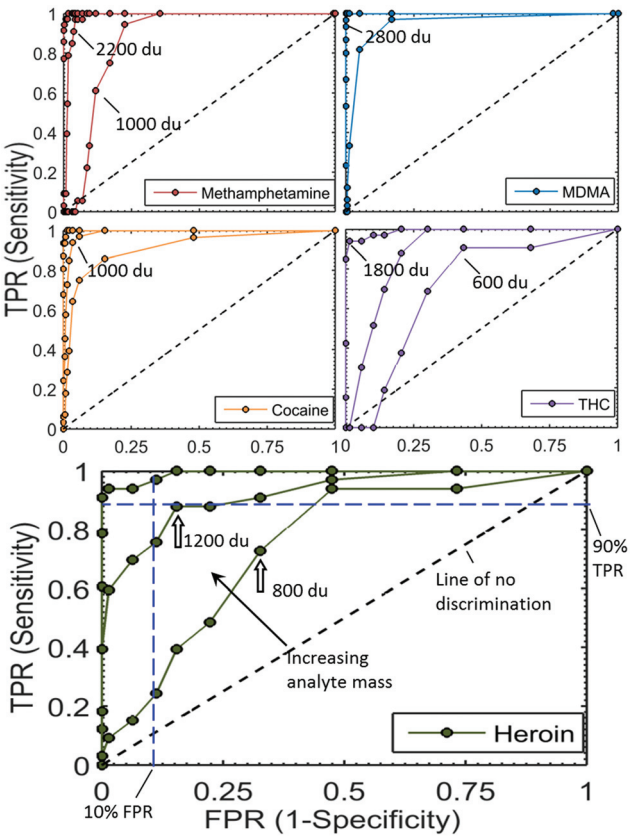


**Fig. 4** ROC curves for each target narcotic at three mass loading levels (methamphetamine: (0.2, 1, 5) ng, MDMA: (1, 5, 15) ng, cocaine: (0.5, 1, 5) ng, THC: (0.5, 2, 5) ng, heroin: (2.5, 10, 25) ng) for IMS operating in Mode 2 with a ±0.05 ms drift time window. Nuisance/alarm thresholds were varied from 0 du to 4000 du in 200 du increments.

ROC curves for THC at 2 ng and 5 ng in both Modes 1 and 2 (Fig. 5).

In addition, ROC curves have previously been used to determine the operational limits of detection for a sensor.[34,36] The ROC curve approach defines detection in terms of the instrument or sensor's ability to differentiate the target from the environmental background experienced under real testing. The limit of detection (LOD) has a number of definitions, including the commonly used target mass for which the instrument/sensor signal is 3× the corresponding noise. In these instances, the noise has often been defined from blank measurements. The results presented here clearly demonstrated the limitations of this definition. Methamphetamine exhibited strong signal intensity for all three masses investigated under controlled laboratory conditions (Mode 1 – Fig. S-5‡), however, given the significant environmental background signal in that drift time; the ROC curve demonstrated relatively modest detection capabilities with a high rate of false positives. The limit of detection, based on a ROC curve approach, can be directly assigned based on the application and user risk aversion by specifying a set TPR and FPR. The IUPAC (International Organization of Pure and Applied Chemistry) defines the default LOD as a TPR of 0.95 and FPR of 0.05, however, other applications such as CWA sensors may specify a TPR of 0.9999 and a FPR of 0.0001. Table 3 summarizes the IMS response for the five selected narcotics under Mode 1 and 2 conditions, targeting a detection rate of ~90% (TPR) while minimizing FPR (targeting <10% FPR) for demonstrative purposes. MDMA, cocaine, and THC all demonstrated single nanogram sensitivity resulting in TPRs ~90% with single-digit FPRs in both Mode 1 and 2 (Table 3). MDMA and cocaine exhibited improvements in the detection limit for Mode 2 conditions (both TPR and FPR) and clearly identified the need for alarm thresholds specific to each set of instrument parameters. On the contrary and as discussed in detail above, though the increased temperatures and sampling time in Mode 2 improved THC desorption/detection, they also increased the relative background in the THC window. Therefore, relatively minimal improvement in the overall IMS response and discrimination capability was observed between modes for THC (Fig. 5(b) and Table 3).

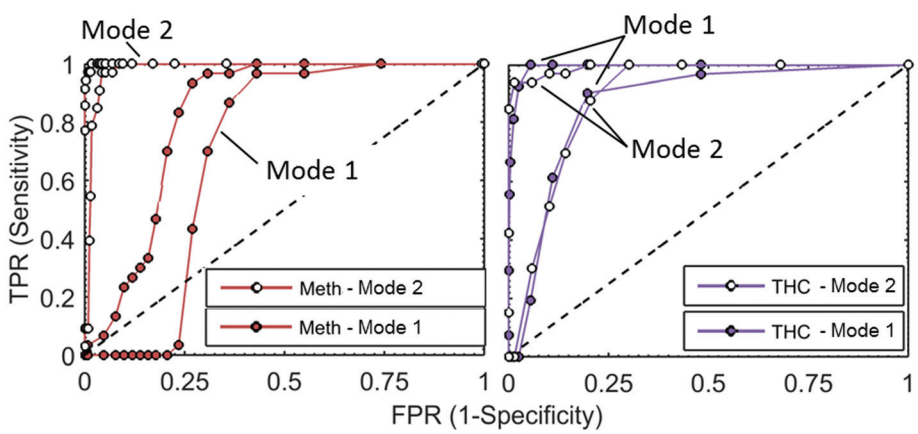


**Fig. 5** ROC curves for methamphetamine (1 ng and 5 ng) and THC (2 ng and 5 ng) in both Mode 1 (filled circles) and Mode 2 (open circles) operating modes.

Table 3 IMS TPR and FPR for illicit narcotics targeting ~90% detection sensitivity (TPR) and minimizing FPR. Target analyte mass, alarm threshold, TPR, and FPR are listed for Mode 1 followed by Mode 2 operating conditions

| Analyte (Mode) | Mass (ng) | Alarm threshold | TPR (%) | FPR (%) |
|---|---|---|---|---|
| METH (1) | 10 | 2000 | 90.0 | 17.8 |
| (2) | 1 | 2200 | 90.0 | 3.8 |
| MDMA (1) | 6 | 1600 | 90.3 | 0.1 |
| (2) | 5 | 2800 | 93.3 | 0.0 |
| Cocaine (1) | 3 | 1600 | 89.3 | 8.2 |
| (2) | 1 | 1000 | 93.9 | 3.5 |
| THC (1) | 5 | 1200 | 92.6 | 2.5 |
| (2) | 5 | 1800 | 93.9 | 1.5 |
| Heroin (1) | 50 | 600 | 90.6 | 18.2 |
| (2) | 10 | 1200 | 87.9 | 15.4 |

Both methamphetamine and heroin displayed sensitivities in the tens of nanogram to achieve 90% TPR in Mode 1, however, for the masses and thresholds specified in Table 3, FPRs near 20% resulted. The Mode 2 operating parameters resulted in significant reduction in the high intensity background in the methamphetamine window, drastically improving the sensitivity down to 1 ng and reducing the FPR under 4%. Similar to THC, the improvements in the heroin signal in Mode 2 were partially offset by the increased level of environmental background. The heroin sensitivity improved; however, there was modest reduction in the FPR (Table 3).

In the base case analysis reported here, a ±0.05 ms window around the measured drift time was used to process the collected environmental background data. The appropriate size of this window was investigated with respect to each compound and mass loading (Fig. S-10–S-13‡). Additional discussion of the drift time window trends can be found in the ESI.‡

All results presented for this investigated were based on an arbitrary sensitivity and specificity target used for demonstrative purposes. Similarly, the response for the two instruments did not precisely match, skewing the results toward better potential discrimination. Clearly from Fig. 3 and 5, the effective limits of detection for each compound will also be dependent on the application's TPR and FPR requirements. In addition, as the environmental background may vary across arenas, this methodology enables the conscious control of the alarm threshold to achieve the desired discrimination between target and background. Finally, it is important to note that we considered pure reference materials for this investigation and illegally produced narcotics may be impure and contain additional contaminants that reduce the discriminative potential. Real samples may also include collected background compounds that may interact during the desorption and ionization processes. Practical limitations (*e.g.*, an inability to dope target analytes onto private vehicles) and the DARPA study recommendations[44] led to the presented methodology to demonstrate relative impact of various parameters and potential discriminative capabilities.

# Conclusions

A number of security agencies employ IMS for the detection and identification of contraband materials, including illicit narcotics. IMS provides sensitive detection, but limitations in selectivity and resolution account for increased rates of nuisance alarms. Here, a ROC curve framework was implemented to evaluate the performance of IMS to detect five illicit narcotics relative to environmental background conditions. Environmental background was assessed from over 20 000 samples collected during the screening of delivery vehicles at a federal facility over a multiyear period. ROC curves were utilized to demonstrate the importance environmental background levels play in the detection of methamphetamine, MDMA, cocaine, THC, and heroin. The capabilities of IMS to discriminate between the target analyte and environmental background was investigated as a function of system parameters (desorber and drift tube temperatures and sampling time) and data processing parameters (alarm threshold, target drift time window, and mass loading). The implementation of ROC curves demonstrated the significant effect environmental background has on the sensitivity and specificity of IMS trace detection. The particular distribution of environmental background for each screening arena must be considered when evaluating the detection and discriminative potential of a methodology.

# Acknowledgements

The U.S. Department of Homeland Security Science and Technology Directorate sponsored a portion of the production of this material under Interagency Agreement IAA HSHQPM-15-T-00050 with the National Institute of Standards and Technology.

# Notes and references

1 H. Thielemann and F. Groh, *Pharmazie*, 1975, **30**, 255–256.
2 S. Joseph, *Chromatographic Methods of Analysis: Thin Layer Chromatography*, Taylor & Francis, 2013.
3 K. Narayanaswami, H. C. Golani and R. D. Dua, *Forensic Sci. Int.*, 1979, **14**, 181–190.
4 D. Furmanec, *J. Chromatogr., A*, 1974, **89**, 76–79.
5 G. R. Nakamura, T. T. Noguchi, D. Jackson and D. Banks, *Anal. Chem.*, 1972, **44**, 408–410.
6 S. Seidi, Y. Yamini, A. Heydari, M. Moradi, A. Esrafili and M. Rezazadeh, *Anal. Chim. Acta*, 2011, **701**, 181–188.
7 R. S. Schwartz and K. O. David, *Anal. Chem.*, 1985, **57**, 1362–1366.
8 M. Krogh, S. Brekke, F. Tønnesen and K. E. Rasmussen, *J. Chromatogr., A*, 1994, **674**, 235–240.
9 Y. T. Iwata, H. Inoue, K. Kuwayama, T. Kanamori, K. Tsujikawa, H. Miyaguchi and T. Kishi, *Forensic Sci. Int.*, 2006, **161**, 92–96.

10 E. S. Chernetsova and G. E. Morlock, *Mass Spectrom. Rev.*, 2011, **30**, 875–883.
11 T. P. Forbes, T. M. Brewer and G. Gillen, *Analyst*, 2013, **138**, 5665–5673.
12 H. Inoue, H. Hashimoto, S. Watanabe, Y. T. Iwata, T. Kanamori, H. Miyaguchi, K. Tsujikawa, K. Kuwayama, N. Tachi and N. Uetake, *J. Mass Spectrom.*, 2009, **44**, 1300–1307.
13 D. J. Weston, R. Bateman, I. D. Wilson, T. R. Wood and C. S. Creaser, *Anal. Chem.*, 2005, **77**, 7572–7580.
14 T. P. Forbes and E. Sisco, *Analyst*, 2014, **139**, 2982–2985.
15 National Institute of Justice, 2000, NIJ Standard 0604.01.
16 S. Bell, *Forensic Chemistry*, Pearson Prentice Hall, New Jersey, 2006.
17 M. Najarro, M. E. Davila Morris, M. E. Staymates, R. Fletcher and G. Gillen, *Analyst*, 2012, **137**, 2614–2622.
18 J. Kozole, J. Tomlinson-Phillips, J. R. Stairs, J. D. Harper, S. R. Lukow, R. T. Lareau, H. Boudries, H. Lai and C. S. Brauer, *Talanta*, 2012, **99**, 799–810.
19 R. G. Ewing, D. A. Atkinson, G. A. Eiceman and G. J. Ewing, *Talanta*, 2001, **54**, 515–529.
20 G. Reid Asbury, J. Klasmeier and H. H. Hill Jr., *Talanta*, 2000, **50**, 1291–1298.
21 J. R. Verkouteren, J. Lawrence, G. A. Klouda, M. Najarro, J. Grandner, R. M. Verkouteren and S. J. York, *Analyst*, 2014, **139**, 5488–5498.
22 G. R. Asbury, C. Wu, W. F. Siems and H. H. Hill Jr., *Anal. Chim. Acta*, 2000, **404**, 273–283.
23 P. Rearden and P. B. Harrington, *Anal. Chim. Acta*, 2005, **545**, 13–20.
24 S. Zimmermann, S. Barth, W. K. M. Baether and J. Ringer, *Anal. Chem.*, 2008, **80**, 6671–6676.
25 T. Khayamian, M. Tabrizchi and M. T. Jafari, *Talanta*, 2006, **69**, 795–799.
26 J. R. Verkouteren and J. L. Staymates, *Forensic Sci. Int.*, 2011, **206**, 190–196.
27 L. T. Demoranville and J. R. Verkouteren, *Talanta*, 2013, **106**, 375–380.
28 A. H. Lawrence, *Forensic Sci. Int.*, 1987, **34**, 73–83.
29 G. A. Eiceman and Z. Karpas, *Ion Mobility Spectrometry*, CRC Press, Boca Raton, FL, 2005.
30 G. A. Eiceman and J. A. Stone, *Anal. Chem.*, 2004, **76**, 390 A–397 A.
31 K. Cottingham, *Anal. Chem.*, 2003, **75**, 435 A–439 A.
32 G. A. Eiceman, W. Yuan-Feng, L. Garcia-Gonzalez, C. S. Harden and D. B. Shoff, *Anal. Chim. Acta*, 1995, **306**, 21–33.
33 I. Cotte-Rodriguez, D. R. Justes, S. C. Nanita, R. J. Noll, C. C. Mulligan, N. L. Sanders and R. G. Cooks, *Analyst*, 2006, **131**, 579–589.
34 C. G. Fraga, A. M. Melville and B. W. Wright, *Analyst*, 2007, **132**, 230–236.
35 C. C. Mulligan, D. R. Justes, R. J. Noll, N. L. Sanders, B. C. Laughlin and R. G. Cooks, *Analyst*, 2006, **131**, 556–567.
36 A. Wysoczanski and E. Voigtman, *Spectrochim. Acta, Part B*, 2014, **100**, 70–77.
37 L. A. Adams, M. Bulsara, E. Rossi, B. DeBoer, D. Speers, J. George, J. Kench, G. Farrell, G. W. McCaughan and G. P. Jeffrey, *Clin. Chem.*, 2005, **51**, 1867–1873.
38 D. Faraggi, B. Reiser and E. F. Schisterman, *Stat. Med.*, 2003, **22**, 2515–2527.
39 C. Heeschen, B. U. Goldmann, L. Langenbrink, G. Matschuck and C. W. Hamm, *Clin. Chem.*, 1999, **45**, 1789–1796.
40 T. C. Martin, J. Moecks, A. Belooussov, S. Cawthraw, B. Dolenko, M. Eiden, J. von Frese, W. Kohler, J. Schmitt, R. Somorjai, T. Udelhoven, S. Verzakov and W. Petrich, *Analyst*, 2004, **129**, 897–901.
41 M. S. Pepe, *The statistical evaluation of medical tests for classification and prediction*, Oxford, New York, NY, 2003.
42 K. H. Zou, W. J. Hall and D. E. Shapiro, *Stat. Med.*, 1997, **16**, 2143–2156.
43 M. H. Zweig and G. Campbell, *Clin. Chem.*, 1993, **39**, 561–577.
44 J. Carrano, in *DARPA Microsystems Technology Office*, U.S. Department of Defense, Washington, DC, 2004.
45 A. J. Jenkins, *Forensic Sci. Int.*, 2001, **121**, 189–193.
46 A. Cecinato and C. Balducci, *J. Sep. Sci.*, 2007, **30**, 1930–1935.
47 C. Postigo, M. J. Lopez de Alda, M. Viana, X. Querol, A. Alastuey, B. Artiñano and D. Barceló, *Anal. Chem.*, 2009, **81**, 4382–4388.
48 M. Viana, X. Querol, A. Alastuey, C. Postigo, M. J. L. de Alda, D. Barceló and B. Artíñano, *Environ. Int.*, 2010, **36**, 527–534.
49 A. Jenkins, *US Patent* 5200614, 1993.
50 A. Jenkins and W. J. McGann, *US Patent* 5491337, 1996.
51 C. L. Crawford, H. Boudries, R. J. Reda, K. M. Roscioli, K. A. Kaplan, W. F. Siems and H. H. Hill, *Anal. Chem.*, 2010, **82**, 387–393.
52 J. E. Parmeter, D. W. Murray and D. W. Hannum, *U.S. Department of Justice*, 2000, NIJ Guide 601-00.
53 G. Kaur-Atwal, G. O'Connor, A. Aksenov, V. Bocos-Bintintan, C. L. Paul Thomas and C. Creaser, *Int. J. Ion Mobility Spectrom.*, 2009, **12**, 1–14.
54 G. A. Eiceman, E. G. Nazarov and J. A. Stone, *Anal. Chim. Acta*, 2003, **493**, 185–194.